Co-evolutionary dynamics between public good producers and cheats in the bacterium *Pseudomonas aeruginosa*

Rolf Kümmerli[1,2], Lorenzo A. Santorelli[3], Elisa Granato[1], Zoé Dumas[2,4], Akos Dobay[5], Ashleigh S. Griffin[3], Stuart A. West[3]

[1] Microbial Evolutionary Ecology, Institute of Plant Biology, University of Zürich, Winterthurerstrasse 190, 8057 Zürich, Switzerland.

[2] Environmental Microbiology, Swiss Federal Institute of Aquatic Science and Technology (Eawag), Überlandstrasse 133, 8600 Dübendorf, Switzerland.

[3] Department of Zoology, University of Oxford, South Parks Road, Oxford OX1 3PS, UK.

[4] Department of Ecology and Evolution, University of Lausanne, Biophore Building, 1015 Lausanne, Switzerland.

[5] Institute of Evolutionary Biology and Environmental Studies, University of Zürich, Winterthurerstrasse 190, 8057 Zürich, Switzerland.

Correspondence: Rolf Kümmerli, email: rolf.kuemmerli@uzh.ch, phone: +41 44 635 2907, fax: +41 44 635 2920

Running title: Co-evolution in bacterial populations

This document is the accepted manuscript version of the following article:
Kümmerli, R., Santorelli, L. A., Granato, E. T., Dumas, Z., Dobay, A., Griffin, A. S., & West, S. A. (2015). Co-evolutionary dynamics between public good producers and cheats in the bacterium Pseudomonas aeruginosa. Journal of Evolutionary Biology, 28(12), 2264-2274. https://doi.org/10.1111/jeb.12751

Abstract

The production of beneficial public goods is common in the microbial world, and so is cheating – the exploitation of public goods by non-producing mutants. Here, we examine co-evolutionary dynamics between cooperators and cheats and ask whether cooperators can evolve strategies to reduce the burden of exploitation, and whether cheats in turn can improve their exploitation abilities. We evolved cooperators of the bacterium *Pseudomonas aeruginosa*, producing the shareable iron-scavenging siderophore pyoverdine, together with cheats, defective in pyoverdine production but proficient in uptake. We found that cooperators managed to co-exist with cheats in 56% of all replicates over approximately 150 generations of experimental evolution. Growth and competition assays revealed that co-existence was fostered by a combination of general adaptions to the media and specific adaptions to the co-evolving opponent. Phenotypic screening and whole-genome re-sequencing of evolved clones confirmed this pattern, and suggest that cooperators became less exploitable by cheats because they significantly reduced their pyoverdine investment. Cheats, meanwhile, improved exploitation efficiency through mutations blocking the costly pyoverdine-signalling pathway. Moreover, cooperators and cheats evolved reduced motility, a pattern that likely represents adaptation to laboratory conditions, but at the same time also affects social interactions by reducing strain mixing and pyoverdine sharing. Overall, we observed parallel evolution, where co-existence of cooperators and cheats was enabled by a combination of adaptations to the abiotic and social environment and their interactions.

Keywords: microbial cooperation, siderophores, experimental evolution, antagonism, cheating resistance, whole-genome resequencing

Introduction

Bacteria frequently cooperate by forming multicellular fruiting bodies and biofilms, and by secreting shareable metabolites to digest food, scavenge essential metals, and attack competitors (West *et al.*, 2007; Nadell *et al.*, 2009; Velicer & Vos, 2009; Strassmann & Queller, 2011). These cooperative traits are typically beneficial for the community, but can also be exploited by cheating mutants that stop contributing to costly cooperation, whilst still capitalizing on the cooperative acts performed by others (West *et al.*, 2006). This raises the question of how cooperation can be maintained given the pervasive risk of cheat exploitation. Previous studies have identified a number of ecological and social factors, including resource availability (Brockhurst *et al.*, 2008; Kümmerli *et al.*, 2009c; Xavier *et al.*, 2011), limited dispersal (Griffin *et al.*, 2004; Gilbert *et al.*, 2007; MacLean & Brandon, 2008; Kümmerli *et al.*, 2009b) and cell density (Greig & Travisano, 2004; Ross-Gillespie *et al.*, 2009), that can tip the balance in favour of cooperation. In contrast to these extrinsic drivers of cooperation, relatively little is known on whether cooperators and cheats can directly adapt to one another, and co-exist under conditions that would normally favour cheating (Zhang *et al.*, 2009; Khare *et al.*, 2009; Hollis, 2012; Levin *et al.*, 2015).

Here, we investigate whether cooperators and cheats co-evolve, eventually engaging in antagonistic co-evolution, as it is typically observed in host-parasite interactions (Decaestecker *et al.*, 2007; Schulte *et al.*, 2010; Gomez & Buckling, 2011; Morran *et al.*, 2011; Thrall *et al.*, 2012). In cooperative systems, cheats can behave analogous to parasites, such that similar evolutionary dynamics might arise. For instance, cooperators could adapt to the presence of cheats by: (a) an obligate reduction in cooperation; (b) a facultative reduction in cooperation when encountering cheats; or (c) making the cooperative trait less exploitable (Khare *et al.*, 2009; Manhes & Velicer, 2011; Ghoul *et al.*, 2014a; Levin *et al.*, 2015). Cheats, meanwhile, could counter-adapt by: (d) evading any form of cheat recognition required for (b); or (e) improving their access to cooperators and their beneficial acts. In addition, it is also possible that cooperators and cheats adapt to abiotic conditions, which might allow social

traits to hitchhike along with beneficial non-social mutations (Morgan *et al.*, 2012; Waite & Shou, 2012; Asfahl *et al.*, 2015).

We examined these possibilities by investigating the evolutionary response of repeatedly interacting cooperator and cheat strains to one another and to the abiotic environment in the bacterium *Pseudomonas aeruginosa*. Specifically, we co-evolved a producer of the shareable iron-scavenging molecule pyoverdine (i.e. cooperator) with a mutant that is defective in pyoverdine production but proficient in uptake (i.e. cheat) in iron-depleted media, where pyoverdine is important for growth. Pyoverdine is produced and secreted by *P. aeruginosa* in response to iron limitation, and is used to scavenge insoluble or host-bound iron from the environment (Schalk & Guillon, 2013). Numerous experiments have shown that secreted pyoverdine molecules can be shared with other cells in the community, including non-producing 'cheats' (Griffin *et al.*, 2004; Harrison *et al.*, 2006; Jiricny *et al.*, 2010; Dumas & Kümmerli, 2012).

We co-evolved populations of cooperators and cheats for 25 rounds of growth (approximately 150 generations), and followed cooperator frequency, population growth and pyoverdine production levels over time. Following evolution, we analysed evolved clones from different time points by using a combination of fitness assays, phenotypic assays, and whole-genome resequencing. This allowed us to examine, both at the proximate and ultimate level, the ability of cooperators and cheats to adapt to each other, and to disentangle co-evolutionary dynamics from adaptations to the abiotic environment.

Materials and Methods

Strains

We used *P. aeruginosa* PAO1 (ATCC 15692) as the wildtype cooperator strain, and the pyoverdine knock-out mutant PAO1Δ*pvdD* (lacking the gene for the pyoverdine synthetase PvdD) as the cheating strain (Ghysels *et al.*, 2004). To be able to distinguish cooperators

from cheats during co-evolution, we used variants of these strains constitutively expressing the green fluorescent protein GFP (PAO1-*gfp* and PAO1Δ*pvdD*-*gfp*, chromosomal insertion: *att*Tn7::Ptac-*gfp*).

Experimental co-evolution

Prior to experimental evolution, we grew strains overnight in 10 ml Lysogeny broth (LB). We then standardized cultures for cell density (optical density OD at 600 nm), and prepared two 1:1 strain mixes (mix1: PAO1-*gfp* vs. PAO1Δ*pvdD*; mix2: PAO1 vs. PAO1Δ*pvdD*-*gfp*, to control for GFP-marker effects). We started experimental evolution by adding 10^6 cells into 1.5 ml iron-depleted CAA medium in 16-fold replication (eight replicates for each mix) on a 24-well plate. Iron-depleted CAA medium contained 5 g/l casamino acids, 1.18 g/l K_2HPO_4*$3H_2O$, 0.25 g/l $MgSO_4$*$7H_2O$, 100 µg/ml human apo-transferrin, 20 mM $NaHCO_3$ and 25 mM HEPES buffer (all from Sigma-Aldrich, Switzerland). Apo-transferrin is a powerful natural iron chelator, which we used to bind ferric iron in the CAA media, thereby preventing siderophore-independent iron uptake. After a 24 hours growth period under static conditions at 37°C, during which approximately six generations occur (Dumas & Kümmerli, 2012), we carried out the following experimental steps: (i) we measured OD (at 600 nm) and pyoverdine production (fluorescence at excitation | emission = 400 | 460 nm) using a multimode plate reader (Tecan Infinite M200 PRO, Tecan Group Ltd., Switzerland) (Kümmerli *et al.*, 2009c); (ii) we diluted culture aliquots to appropriate levels in 0.8 % NaCl, and plated 30 µl onto LB agar containing 100 µM $FeCl_3$ to assess strain frequency ($FeCl_3$ was supplemented to suppress residual pyoverdine production, which can interfere with the GFP-signal); (iii) mixed 200 µl of the culture with 100 µl LB and 100 µl glycerol for long-term storage at -80°C; and (iv) transferred 15 µl of the culture to fresh medium (corresponding to a 100-fold dilution) to initiate the next round of growth. We counted colony-forming units (CFU) on LB agar plates following a 48 h incubation period (24 h at 37°C followed by 24h at room temperature). We differentiated GFP-tagged from non-tagged colonies using a Dark Reader Transilluminator (Clare Chemical Research, US). The above procedure was repeated for 25

consecutive rounds of growth, resulting in approximately 150 generations of experimental co-evolution.

Time-shift competition assays

In order to test whether evolved cooperators became better at coping with cheats, and/or evolved cheats improved their ability to exploit cooperators, we competed ancestral and evolved clones from various time points against each other in all possible pairwise combinations. Specifically, we isolated a total of 896 clones (on average 8.8±1.8 and 9.5±1.2 clones of cooperator and cheat origin, respectively) from the 5^{th}, 10^{th}, 15^{th}, 20^{th}, and 25^{th} round of growth. This was possible for 11 of the 16 replicates, where the two strains co-existed for most of the experimental period (i.e. 3 replicates until 20^{th} round; 8 replicates until 25^{th} round). In the other five replicates, cheats completely displaced cooperators, which concomitantly resulted in population collapse and extinction. For each round-replicate combination, we grew the isolated clones individually in 96-well plates in CAA without apo-transferrin, conditions under which all clones reached similar OD after 24 hours (mean OD ± SE = 0.460±0.007). We then mixed equal volumes (50 µl) of all cooperator or cheat clones originating from the same round-replicate combination in Eppendorf tubes. With these mixes, we set up 1:1 competitions between cooperators and cheats in all possible pairwise combinations, such that cooperators competed against cheats from their past, presence and future. Following a 24 h competition period in iron-depleted CAA medium under static conditions at 37°C, we plated appropriately diluted fractions of the competition cultures onto LB plates. Following a 48 h incubation period, we counted the GFP-tagged versus non-tagged strains as described above. Using CFU data, we calculated the relative fitness of cheats as $v = [x_2(1-x_1)]/[x_1(1-x_2)]$, where x_1 and x_2 are the starting and final frequency of cheats in the population, respectively. x_1 was based on the ratios of the OD of the starting cultures, and was typically close to 0.5. We log-transformed all fitness values prior to analysis to obtain normally distributed residuals.

Growth and competition assays to test for adaptation to the media and/or the social environment

We first tested for adaptation to the laboratory (abiotic) environment by growing monocultures of all 896 clones used for the time-shift competition assay in the medium they have evolved in (i.e. iron-depleted CAA). If clones significantly improve their growth performance in this assay, then this would indicate that strains have adapted to abiotic conditions. We measured OD at 600 nm of all clones after a 24 h static growth assay at 37°C. OD after 24 hours is a good proxy for fitness under the strongly growth-limiting conditions imposed in our experiment because strains grow slowly, linearly over time, and do not reach carrying capacity within 24 hours (see Supporting Information Fig. S1 and (Kümmerli *et al.*, 2009c). Thus, any beneficial mutation shortening the lag phase and/or increasing growth rate will result in higher OD. We scaled ODs of evolved strains relative to the ancestral wildtype.

In addition to these clonal assays, we competed evolved cooperator and cheat clones (from the end of the co-evolution) directly against their respective ancestors in mixed culture (using the same protocol as described above). For this assay, it is important to note that competitive ability can still be influenced by both abiotic and social adaptations. Thus, if evolved cooperators were found to outcompete their ancestors, this could result from adaptation to media, as well as from the opportunity to exploit any surplus pyoverdine produced by ancestral strains. To disentangle social from abiotic fitness effects, we performed competition assays in iron-deplete media, where both social and abiotic adaptations should play a role, and iron-replete media, where pyoverdine is not needed and therefore only abiotic adaptations should matter.

Another possibility to implement control treatments would have been to evolve cooperator and cheat strains in isolation from each other (Brockhurst & Koskella, 2013). However, this is difficult with our system because cheat monocultures grow poorly, such that these cultures

would have likely gone extinct during the serial passages of the evolution regime (Supporting Information Fig. S2, and also see (Fiegna & Velicer, 2003). Furthermore, *de novo* cheats arise quickly in cooperator monocultures (Harrison *et al.*, 2008; Dumas & Kümmerli, 2012), such that this treatment would have turned from a control into a co-evolution treatment.

Sequencing and SNP analysis

We sequenced the entire genome of 90 cooperator and 105 cheat clones from the end of the experimental co-evolution (R25 for 8 replicates, and R20 for 3 replicates) using Illumina HiSeq 2000. The evolved 195 clones were arranged in 30 pools as listed in Table S1 (Supporting Information). We pooled the cheat clones originating from the same replicate (11 pools in total). The cooperator clones were also pooled per replicate but also based on phenotypes. Specifically, we identified clones with significantly altered pyoverdine production levels in some replicates. For these replicates, we assembled the clones with and without changed pyoverdine production levels in separate pools (19 pools in total). Finally, we also sequenced our ancestral wildtype strain PAO1.

We extracted genomic DNA using the Wizard Genomic DNA purification kit (Promega, Switzerland). Extracted DNA was sent off for commercial library preparation and sequencing with Illumina HiSeq 2000 using paired-end 50-bp reads (paired-end and single reads for 20 and 11 pools, respectively; GATC Biotech, Germany). Data analysis was performed in collaboration with the Genetic Diversity Centre (GDC), ETH Zurich. In a first step, we mapped the contigs of our wildtype strain onto the reference genome of PAO1 (Stover *et al.*, 2000), PAO1-UW http://pseudomonas.com/index.jsp). The average sequence coverage was high (222), and the consensus length of our re-sequenced wildtype strain was 99.985% of the reference genome (6,264,404 bp). Reference and re-sequenced wildtype strain differed in 25 SNPs (10 non-synonymous, 5 synonymous, and 10 intergenic SNPs, see Supporting Information Table S2). Next, we mapped the contigs of our evolved clones onto the re-sequenced genome of our ancestral wildtype strain. Whenever a single clone was

sequenced, we considered a putative mutation as a SNP if its frequency was ≥ 80%. In cases where clones were pooled for sequencing, we used the following threshold frequencies for putative mutations to be considered as SNPs (for 2 clones: frequency ≥ 25%, for 3 clones: frequency ≥ 16.7%, for 4 clones: frequency ≥ 12.5%, for 5 clones: frequency ≥ 10%, for 6 clones: frequency ≥ 8.3%, for 7 clones: frequency ≥ 7.1%, for 8 clones: frequency ≥ 6.3%, for 9 clones: frequency ≥ 5.6%, for 10 clones: frequency ≥ 5%). We discarded putative mutations with coverages < 15. Using these criteria, we identified 62 non-synonymous SNPs in coding DNA sequences, and 19 SNPs in intergenic regions (Supporting Information Table S1).

Swarming assays

Because we identified SNPs in genes involved in flagella synthesis and chemotaxis (Table S1, for cooperators in 8 out of 11 replicates; for cheats in 9 out of 11 replicates), we tested whether clones isolated from pools with such SNPs showed altered motility phenotypes. For this analysis, we focused on a subset of samples (5 cooperator and cheat pools each). For each of the 31 cooperator and 45 cheat clones from these pools, we quantified swarming motility on 0.4% LB agar in 3-fold replication. Specifically, we grew clones overnight in 10 ml LB medium at 200 rpm at 37°C. We then washed cells in PBS (phosphate buffer saline), adjusted OD to 1, and added 2 µl of the cell solution to the centre of a Petri dish containing 20 ml 0.4% LB agar. Dishes were incubated statically for 24 h at 37°C. Following incubation, the dishes were placed individually on 1 mm grid paper and photographed. We analysed the pictures with GIMP 2.8 (GNU Image Manipulation Program, freely available from http://www.gimp.org), by quantifying the number of pixels covered by the swarming colony. The 1 mm grid was used to calculate the surface s (in cm^2) covered by the swarm. We then calculated the relative swarming of evolved strains as $r_s = (s_{evolved}-s_{PAO1\Delta rhlA})/(s_{PAO1}- s_{PAO1\Delta rhlA})$, where $s_{evolved}$, s_{PAO1}, $s_{PAO1\Delta rhlA}$ are the swarm surfaces of the evolved, ancestral wildtype, and a swarming-knockout strain (PAO1Δ*rhlA*, which lacks the gene for the production of

rhamnolipids, biosurfactants essential for swarming), respectively. Evolved strains were considered swarming impaired if $r_s < 0.75$.

Simulating the effect of motility impairment on pyoverdine sharing

SNPs in motility genes most likely represent adaptation to laboratory conditions (Ritchings *et al.*, 1995; Velicer *et al.*, 1998). However, motility deficiency potentially feeds back on social interactions between cooperators and cheats by limiting strain mixing, which in turn can reduce the cheats' access to pyoverdine (see Kümmerli *et al.*, 2009b). Because such a feedback is difficult to examine experimentally, we used a simulation platform specifically designed to study social interactions in microbes (Dobay *et al.*, 2014). This platform provides a two-dimensional continuous landscape, in which public-goods-producing cooperators and non-producing cheats are seeded. Simulations typically start with one cooperator and one cheat cell, and stop when populations reach the carrying capacity K (number of individuals). Cooperator cells produce public good molecules at a specified rate p (molecules per second) and with specific properties (diffusion coefficient D_{pg} and durability δ). Public good production (per molecule) comes at a cost c, whereas public good uptake generates a benefit b. Cooperator and cheats can themselves diffuse (i.e. are motile), whereby D_{co} and D_{ch} describe their respective diffusion coefficients. The fitness functions of cooperators and cheats are described in detail in Dobay et al. (2014), and are basically the sum of the intrinsic growth rate μ (not influenced by public goods), the benefits generated by public good uptake, and the cost of public goods production accruing to cooperators.

As a baseline for our simulations, we chose parameter settings that closely match our experimental system – a liquid environment where cell and public good diffusion is relatively high, and where public goods are important for growth ($p = 1$, $D_{pg} = 5\ \mu m^2 s^{-1}$, $\delta = 510$ s, $c = 0.001$, $b = 0.01$, $D_{co} = D_{ch} = 5\ \mu m^2 s^{-1}$, $\mu = 1$, $K = 500$). With these settings, cheats significantly outcompete cooperators, demonstrating the fact that cheats can free ride on the public goods produced by cooperators. To investigate how motility impairment (as observed in our

experiment) feedbacks on the relative success of cooperators and cheats, we simulated situations in which cooperators and/or cheats acquire mutations reducing their cell diffusion coefficient from $D_{co} = D_{ch} = 5$ to 0.5 $\mu m^2 s^{-1}$. We simulated two scenarios, one where motility reduction is neutral (constant $\mu = 1$), and one where motility reduction is beneficial, increasing μ by 0.2%. For each parameter combination, we ran 500 independent simulations.

Statistical analysis

We used linear models (LM) and linear mixed models (LMM) for statistical analyses. We tested whether the frequency of cheats, absolute and relative fitness, and levels of pyoverdine production changed over evolutionary time. Furthermore, we tested for correlations between genotypes (SNPs) and phenotypes (growth, pyoverdine production, and motility). Since repeated measures were taken from the same replicates over time, we included replicate ID as a random factor into our model. We also accounted for the fact that clones from the same replicate are not independent by averaging across clones prior to analysis. All statistical analyses were carried out with R 3.1.1 (R Development Core Team, 2015).

Results

Evolutionary dynamics of strain frequency, growth and pyoverdine production

We found that cheats significantly increased in frequency over evolutionary time (LMM: $t_{332} = 10.96$, $P < 0.0001$); average cheat frequency rose rapidly during the first part of the experiment, but then levelled off (Fig. 1a). There was also a significant GFP-marker effect (LMM: $t_{14} = 3.93$, $P = 0.0015$), but only at the beginning of the experiment (significant interaction between round and marker: LMM: $t_{332} = 6.32$, $P < 0.0001$). When looking at individual replicates, we observed that cheats became fixed in 7 out of 16 replicates (fixation events occurred in rounds 13, 21, 23, and 25), whereas cooperators co-existed with cheats across the entire duration of the experiment (mean cheater frequency ± SE = 0.71±0.04) in the remaining 9 replicates.

296 During experimental evolution, both population growth (LMM: t_{382} = -10.16, P < 0.0001, Fig.
297 1b) and population-level pyoverdine production (LMM: t_{382} = -15.41, P < 0.0001,Fig. 1c)
298 significantly decreased over time. When comparing across replicates, we found that end
299 point values of cheat frequency were significantly negatively correlated with evolved
300 population growth (Pearson's product-moment correlation: r = -0.894, df = 14, P < 0.0001),
301 and evolved pyoverdine production levels (r = -0.764, df = 14, P = 0.0006) (Supporting
302 Information Fig. S2), showing that the spreading of cheats typically drives population growth
303 and pyoverdine production towards zero.
304
305 ***Time-shift competition assays suggest co-evolutionary dynamics***
306 Among the replicates where cooperators and cheats co-existed for at least 20 experimental
307 rounds, we found that cooperators from later evolutionary time points performed significantly
308 better in competition with cheats than cooperators from earlier time points (Fig. 2a-f; LM: t_{319}
309 = -4.67, P < 0.0001). Similarly, cheats from later evolutionary time points became
310 increasingly better at outcompeting cooperators (Fig. 2a-f), as indicated by the consistent
311 significant positive relationships between cheat round of origin and relative cheat fitness (LM:
312 t_{319} = 5.21, P < 0.0001). In contemporary competitions (i.e. competitions where cooperators
313 and cheats originate from the same round), cheats significantly outcompeted cooperators (t_{58}
314 = 2.06, P = 0.044), suggesting that cooperators remained vulnerable to exploitation at any
315 given moment in time.
316
317 ***Abiotic and social adaptations influence evolutionary dynamics***
318 The competitive advantage of evolved strains in the time-shift experiment could not only
319 have arisen due to social interactions, but also through adaptation to the abiotic environment.
320 Our monoculture experiments, in which we grew evolved cooperator and cheat clones
321 outside the social context, indeed suggest that media adaptation occurred: cooperator and
322 cheat clones slightly but significantly improved their growth over evolutionary time (Fig. 3a,
323 LMM for cooperators: t_{48} = 2.81, P = 0.007; for cheats: t_{48} = 2.17, P = 0.035). However,

another insight gained from these monoculture experiments was that the cooperators' pyoverdine production levels significantly dropped over evolutionary time (Fig. 3b, LMM for cooperators: t_{48} = - 6.43, P < 0.0001), indicating that selection also acted on the social trait of interest. In support of the hypothesis that both social and abiotic adaptations drove the evolutionary dynamics observed in Fig. 2, we found that, in competitions between evolved and ancestral cooperators, the relative fitness of evolved cooperators was significantly higher under iron-deplete conditions, where both social and abiotic adaptations played a role, than under iron-replete conditions, where only abiotic adaptations mattered (Fig. 3c, paired *t*-test: t_9 = 6.93, P < 0.0001). Competitions between ancestral and evolved cheats, meanwhile, were less informative because these cultures hardly managed to grow. But also here, we found evidence for media adaption since the evolved cheats grew slightly but significantly better than their ancestor (mean number of doublings in 24 hours: evolved vs. ancestral cheats = 2.53±0.40 vs. 0.41±0.11, paired *t*-test: t_8 = 6.36, P = 0.0002).

Sequencing analyses reveal mutations in social and non-social genes

To better understand the genetic basis of the observed evolutionary dynamics, we sequenced genomes of 195 evolved clones from the end of the experiment. We found that non-synonymous SNPs repeatedly arose in three functionally different regions of the genome (Table S1), which correspond to: (a) sequences coding and regulating the iron starvation sigma factor *pvdS* (13 putative independent mutation events); (b) sequences coding for various genes involved in flagella synthesis and regulation (16 putative independent mutation events); and (c) sequences coding for genes involved in chemotaxis (11 putative independent mutation events). Intriguingly, mutations in all three regions were found both in the cooperator and the cheat background (number of events in cooperator vs. cheat background for *pvdS* region: 8/5; for flagella genes: 9/7; for chemotaxis genes: 4/7).

352 ***Phenotypes and fitness associated with SNPs in pvdS region***

353 There was a perfect association between reduced levels of pyoverdine production among
354 cooperator clones and the presence of mutations in the *pvdS* region (Table S1). Specifically,
355 clones with *pvdS* mutations showed significantly lower pyoverdine production levels than
356 clones without *pvdS* mutations (pyoverdine production level relative to the ancestral wildtype,
357 mean ± SE, for clones with *pvdS* mutations: 0.25±0.06; without *pvdS* mutations: 0.99±0.04;
358 LM: $F_{1,16} = 95.29$, $P < 0.0001$; Fig. 4). Moreover, the presence/absence of *pvdS* mutations
359 correlated with clonal fitness. Cooperator clones without *pvdS* mutations grew significantly
360 better than clones with *pvdS* mutations (LM: $F_{1,16} = 9.73$, $P = 0.007$), and also better than the
361 ancestral wildtype ($t_9 = 4.07$, $P = 0.0028$, Fig. 4). Evolved clones with *pvdS* mutations varied
362 a lot in their growth performance (in some cases growth decreased dramatically), but overall
363 there was no significant drop in growth relative to the ancestral wildtype ($t_6 = -1.42$, $P =$
364 0.199, Fig. 4).
365
366 Cheat clones with *pvdS* SNPs were phenotypically indistinguishable from the ancestral cheat
367 and typically did not fix (i.e. the sequenced pools consisted of a mix of clones with and
368 without mutations in *pvdS*, Table S1). For those reasons, we could not link mutations to
369 fitness. However, there was one replicate (No. 8, Table S1) in which all sequenced cheat
370 clones had a mutation in the *pvdS* region. These clones showed growth almost identical to
371 their ancestor (mean growth ± SE: 0.99±0.03, $t_9 = 0.29$, $P = 0.78$).
372
373 ***Phenotypes and fitness associated with SNPs in flagella and chemotaxis genes***
374 Across the subset of sequenced pools analysed, we consistently found that the presence of
375 SNPs in flagella and chemotaxis genes went along with the presence of clones showing
376 significantly reduced swarming (mean relative swarming compared to the ancestral wildtype
377 r_s ± SE: 0.374±0.054). Evolved clones with motility impairment grew marginally significantly
378 better than the ancestral wildtype ($t_{10} = 2.06$, $P = 0.066$, Fig. 5), but not significantly different
379 from the evolved strains without motility impairment ($F_{1,15} = 0.40$, $P = 0.537$).

Simulations reveal that motility impairment promotes cooperation

Our experiments were carried out in static liquid medium, where flagellated wildtype bacteria can easily mix and siderophores can readily diffuse. Under such conditions, cheats typically outcompete cooperators (Griffin *et al.*, 2004; Kümmerli *et al.*, 2009b). However, how do the competitive abilities change when strains become motility impaired as observed in our co-evolution experiment? To address this question, we used computer simulations where we could manipulate bacterial motility in a fully controlled *in silico* environment (see Materials and Methods for details). When simulating ancestral conditions, where bacteria are highly motile, we indeed found that cooperators lose in competition with cheats (cooperator frequency drops from 0.5 to 0.256). Next, we implemented our empirical observation that strains became motility impaired. When assuming that motility impairment confers no fitness benefit, our simulations reveal that cooperators increase in frequency, relative to the standard conditions described above, no matter whether motility impairment occurred in cooperators (frequency increase from 0.256 to 0.319), cheats (from 0.256 to 0.264), or both strains (from 0.256 to 0.370). Finally, we simulated the case where motility impairment confers a small fitness benefit and where both strains became motility impaired (as observed in our experiment). Also under these conditions, we found that cooperators increased in relative frequency (from 0.256 to 0.399). These results indicate that motility impairment benefits cooperators more than cheats because it leads to more local sharing of public goods among cooperators.

Discussion

Our co-evolution study with *P. aeruginosa* revealed that pyoverdine-producing cooperators could co-exist with pyoverdine-exploiting cheats across 150 bacterial generations in the majority (56%) of replicates. Our phenotypic and sequencing analyses suggest that co-existence was fostered by cooperators and cheats adapting to both one another and the abiotic environment. Adaptations to the co-evolving opponent included cooperators significantly down-regulating their pyoverdine production, which lowered the overall level of

cooperation, and cheats blocking costly pyoverdine signalling, which is triggered upon pyoverdine uptake. Adaptations to the abiotic environment included a reduction in motility, which could potentially feed back on social interactions between cooperators and cheats by limiting strain mixing and pyoverdine sharing.

We found that an obligate reduction in cooperation by 75%, owing to point mutations in the gene and promoter region of the iron starvation sigma factor PvdS arose repeatedly in many replicates. This illustrates how the presence of cheats can favour public good producers to reduce their level of cooperation (Dumas & Kümmerli, 2012; Ghoul *et al.*, 2014a). However, these partial pyoverdine producers hardly ever fixed, such that populations generally consisted of a mixture of ancestral full-pyoverdine producers, evolved partial-pyoverdine producers and non-producers. The evolved partial-pyoverdine producers could therefore take on a double role in the population: they can be regarded as cooperators in competition with the non-producer, but potentially act as cheats in competition with the ancestral wildtype pyoverdine producer (Ghoul *et al.*, 2014b). Further work is required to determine if this diversity of pyoverdine strategies can remain stable in the long run, by a mechanism such as frequency-dependent selection (Ross-Gillespie *et al.*, 2007; MacLean & Gudelj, 2006; Ross-Gillespie *et al.*, 2015).

We further observed that point mutations in the iron starvation sigma factor region also repeatedly occurred in the cheat background. The spreading of these mutants can be explained by the fact that our ancestral cheat (defective for the pyoverdine synthetase PvdD) is still receptive to pyoverdine-mediated signalling (Lamont *et al.*, 2002), whereby the uptake of pyoverdine triggers the expression of genes involved in the synthesis of pyoverdine precursors. Signalling is silent when cheats grow in monoculture, but becomes activated in co-culture with pyoverdine producers (Tiburzi *et al.*, 2008), consequently leading to substantial costs associated with cheating. These costs can be eliminated by mutations in

435 the iron starvation sigma factor (Tiburzi *et al.*, 2008). Thus, the spreading of these mutations
436 can be understood as a direct response to the presence of cooperators.
437
438 What role do adaptations to the abiotic environment, such as the observed reduction in
439 motility, play in the co-evolutionary dynamics between cooperators and cheats? Previous
440 work suggested that cooperative traits could hitchhike along with mutations that provide
441 benefits outside the social context (Morgan *et al.*, 2012; Waite & Shou, 2012; Asfahl *et al.*,
442 2015). The reasoning is that in cooperative systems cheats must invade from rare, and
443 therefore any beneficial (non-social) mutation is more likely to occur among cooperators
444 because they are more numerous. This could finally result in selective sweeps, during which
445 the beneficial mutation fixes, the cooperative trait hitchhikes along, and cheats are purged
446 (Waite & Shou, 2012). We did not find support for this scenario. For one thing, we started
447 with equal proportions of cooperators and cheats such that hitchhiking could work in favour
448 of both strains depending on in which background the beneficial (non-social) mutation arises
449 first. However, even when taking this into account, we found no clear evidence for hitchhiking
450 based on selective sweeps. One reason for the absence of large-scale hitchhiking might be
451 that motility impairment seems to confer only small fitness benefits (Fig. 5). Moreover,
452 simulations suggest that motility impairment feeds back on the social interaction between
453 cooperators and cheats as it limits strain mixing, which in turn can lead to more local sharing
454 of public goods among cooperators, hampering the selective advantage of cheats. Taken
455 together, our findings indicate that adaptations to the abiotic environment can interact with
456 social components of the environment, and do not necessarily favour hitchhiking.
457
458 Do the observed adaptations indicate that cooperators and cheats engage in antagonistic co-
459 evolution, characterized by cooperators becoming resistant against cheating and cheats
460 improving exploitation abilities? The answer is ‘no’, as we did not observe cooperators to
461 evolve mechanisms preventing public good exploitation whilst maintaining high levels of
462 cooperation. Nonetheless, in our study the evolution of reduced pyoverdine production and

463 the feedback of motility impairment on social interactions significantly helped to reduce the
464 burden of cheating and allowed cooperators to co-exist with cheats for much longer periods
465 than would be expected based on the results from short-term invasion experiments (Griffin *et*
466 *al.*, 2004; Ross-Gillespie *et al.*, 2007; Kümmerli *et al.*, 2009c). Furthermore, the mutations in
467 the iron starvation sigma factor increased the relative fitness of cheats when grown with
468 cooperators that produced pyoverdine. Thus, whilst we did not observe antagonistic co-
469 evolution, we did observe both cooperators and cheats becoming better adapted to a social
470 environment that includes the other type.
471
472 Would the observed response of cooperators, to reduce pyoverdine production and impair
473 motility, help sustain some level of cooperation in the long run? Again, the answer is 'no'.
474 First of all, we observed cheat fixation in 7 out of 16 replicates. This is by itself not surprising
475 because we chose experimental conditions that are highly unfavourable for cooperation, as
476 we combined high costs of cooperation (induced by strong iron limitation) with low
477 relatedness (thousands of cells were transferred and no population structure was
478 implemented) (Griffin *et al.*, 2004; Kümmerli *et al.*, 2009a). Second, even in the remaining 9
479 replicates, where strains co-existed more stably, the long-term persistence of cooperation is
480 not guaranteed, as exemplified by the evolutionary dynamics observed in replicate no. 11
481 (Table S1). In this replicate, a motility-reducing flagella mutation fixed early among
482 cooperator clones, allowing the evolved cooperators to co-exist with cheats. Subsequently,
483 two independent mutations in the iron starvation sigma factor occurred that resulted in the
484 complete abolishment of pyoverdine production, such that the final population consisted of a
485 mixture of ancestral and *de novo* evolved pyoverdine non-producers. Although reflecting an
486 extreme case, this example shows that a single point mutation suffices to turn a reasonably
487 well-adapted cooperator into a *de novo* cheat. These considerations suggest that some form
488 of population structure, generating significant levels of relatedness among interacting
489 individuals (i.e. public goods are more likely shared among cooperators), might be required

to further stabilize cooperation (Griffin *et al.*, 2004; MacLean & Gudelj, 2006; Diggle *et al.*, 2007; Kümmerli *et al.*, 2009a; Rumbaugh *et al.*, 2012).

Finally, we can speculate about whether cheating resistance is possible in our system and what putative mechanisms could confer it. The evolution of cheating resistance combined with sustained high levels of cooperation was indeed observed in a study where only cooperators but not cheats were allowed to evolve (Santorelli *et al.*, in preparation). While the underlying resistance mechanism remained unclear in this particular study, cheating resistance could principally evolve via a modified, more specific pyoverdine that is no longer accessible to cheats. This scenario has indeed previously been put forward to explain the existing pyoverdine diversity (Smith *et al.*, 2005; Lee *et al.*, 2012), and has also been suggested to drive diversification in bacterial quorum-sensing communication systems (Eldar, 2011). One reason for why diversification did not appear in our experiment might be that at least two mutations are required to change pyoverdine specificity – one that alters pyoverdine structure and one that adjusts receptor specificity accordingly. The odds for this to occur within our relatively short experimental period are conceivably low. Thus, the question of whether cooperator-cheat antagonism can drive diversification in social systems remains still open.

Acknowledgments

We thank: Jean-Claude Walser from the Genetic Diversity Center (GDC), ETH Zurich, for help with sequence analysis; the Swiss National Science Foundation (grants no. PZ00P3-126337 and PP00P3-139164) and the ERC for funding.

References

Asfahl, K. L., Walsh, J., Gilbert, K. & Schuster, M. 2015. Non-social adaptation defers a tragedy of the commons in *Pseudomonas aeruginosa* quorum sensing. *ISME J.* in press.

518 Brockhurst, M. A., Buckling, A., Racey, D. & Gardner, A. 2008. Resource supply and the
519 evolution of public-goods cooperation in bacteria. *BMC Biol.* **6**: 20.
520 Brockhurst, M. A. & Koskella, B. 2013. Experimental coevolution of species interactions.
521 *Trends Ecol. Evol.* **28**: 367-375.
522 Decaestecker, E., Gaba, S., Raeymaekers, J. A. M., Stoks, R., Van Kerckhoven, L., Ebert, D.
523 & De Meester, L. 2007. Host-parasite 'Red Queen' dynamics archived in pond
524 sediment. *Nature* **450**: 870-873.
525 Diggle, S. P., Griffin, A. S., Campell, G. S. & West, S. A. 2007. Cooperation and conflict in
526 quorum-sensing bacterial populations. *Nature* **450**: 411-414.
527 Dobay, A., Bagheri, H. C., Messina, A., Kümmerli, R. & Rankin, D. J. 2014. Interaction
528 effects of cell diffusion, cell density and public goods properties on the evolution of
529 cooperation in digital microbes. *J. Evol. Biol.* **27**: 1869-1877.
530 Dumas, Z. & Kümmerli, R. 2012. Cost of cooperation rules selection for cheats in bacterial
531 metapopulations. *J. Evol. Biol.* **25**: 473-484.
532 Eldar, A. 2011. Social conflict drives the evolutionary divergence of quorum sensing. *Proc.*
533 *Natl. Acad. Sci. U.S.A.* **108**: 13635-13640.
534 Fiegna, F. & Velicer, G. J. 2003. Competitive fates of bacterial social parasites: persistence
535 and self-induced extinction of *Myxococcus xanthus* cheaters. *Proc. R. Soc. B* **270**:
536 1527-1534.
537 Ghoul, M., Griffin, A. S. & West, S. A. 2014a. Toward and evolutionary definition of cheating.
538 *Evolution* **68**: 318-331.
539 Ghoul, M., West, S. A., Diggle, S. P. & Griffin, A. S. 2014b. An experimental test of whether
540 cheating is context dependent. *J. Evol. Biol.* **27**: 551-556.
541 Ghysels, B., Thi Min Dieu, B., Beatson, S. A., Pirnay, J.-P., Ochsner, U. A., Vasil, M. L. &
542 Cornelis, P. 2004. FpvB, an alternative type I ferripyoverdine receptor of
543 *Pseudomonas aeruginosa*. *Microbiology* **150**: 1671-1680.

544 Gilbert, O. M., Foster, K. R., Mehdiabadi, N. J., Strassmann, J. E. & Queller, D. C. 2007.
545 High relatedness maintains multicellular cooperation in a social amoeba by controlling
546 cheater mutants. *Proc. Natl. Acad. Sci. U.S.A.* **104**: 8913-8917.
547 Gomez, P. & Buckling, A. 2011. Bacteria-phage antagonistic coevolution in soil. *Science* **332**:
548 106-109.
549 Greig, D. & Travisano, M. 2004. The Prisoner's Dilemma and polymorphism in yeast *SUC*
550 genes. *Biol. Lett.* **Supplements 3**: S25-S26.
551 Griffin, A., West, S. A. & Buckling, A. 2004. Cooperation and competition in pathogenic
552 bacteria. *Nature* **430**: 1024-1027.
553 Harrison, F., Browning, L. E., Vos, M. & Buckling, A. 2006. Cooperation and virulence in
554 acute *Pseudomonas aeruginosa* infections. *BMC Biol.* **4**: 21.
555 Harrison, F., Paul, J., Massey, R. C. & Buckling, A. 2008. Interspecific competition and
556 siderophore-mediated cooperation in *Pseudomonas aeruginosa*. *ISME J.* **2**: 49-55.
557 Hollis, B. 2012. Rapid antagonistic coevolution between strains of the social amoeba
558 *Dictyostelium discoideum*. *Proc. R. Soc. B* **279**: 3565-3571.
559 Jiricny, N., Diggle, S. P., West, S. A., Evans, B. A., Ballantyne, G., Ross-Gillespie, A. &
560 Griffin, A. S. 2010. Fitness correlates with the extent of cheating in a bacterium *J.*
561 *Evol. Biol.* **23**: 738-747.
562 Khare, A., Santorelli, L. A., Strassmann, J. E., Queller, D. C., Kuspa, A. & Shaulsky, G. 2009.
563 Cheater-resistance is not futile. *Nature* **461**: 980-983.
564 Kümmerli, R., Gardner, A., West, S. A. & Griffin, A. S. 2009a. Limited dispersal, budding
565 dispersal and cooperation: an experimental study *Evolution* **63**: 939-949.
566 Kümmerli, R., Griffin, A. S., West, S. A., Buckling, A. & Harrison, F. 2009b. Viscous medium
567 promotes cooperation in the pathogenic bacterium *Pseudomonas aeruginosa*. *Proc.*
568 *R. Soc. B* **276**: 3531-3538.
569 Kümmerli, R., Jiricny, N., Clarke, L. S., West, S. A. & Griffin, A. S. 2009c. Phenotypic
570 plasticity of a cooperative behaviour in bacteria. *J. Evol. Biol.* **22**: 589-598.

571 Lamont, I. L., Beare, P., Ochsner, U., Vasil, A. I. & Vasil, M. L. 2002. Siderophore-mediated
572 signaling regulates virulence factor production in *Pseudomonas aeruginosa*. *Proc.*
573 *Natl. Acad. Sci. U.S.A.* **99**: 7072-7077.
574 Lee, W., van Baalen, M. & Jansen, V. A. A. 2012. An evolutionary mechanism for diversity in
575 siderophore producing bacteria. *Ecol. Lett.* **15**: 119-125.
576 Levin, S. R., Brock, D. A., Queller, D. C. & Strassmann, J. E. 2015. Concurrent co-evolution
577 of intra-organismal cheaters and resisters. *J. Evol. Biol.* **28**: 756-765.
578 MacLean, R. C. & Brandon, C. 2008. Stable public goods cooperation and dynamic social
579 interactions in yeast. *J. Evol. Biol.* **21**: 1836-1843.
580 MacLean, R. C. & Gudelj, I. 2006. Resource competition and social conflict in experimental
581 populations of yeast. *Nature* **441**: 498-501.
582 Manhes, P. & Velicer, G. J. 2011. Experimental evolution of selfish policing in social bacteria.
583 *Proc. Natl. Acad. Sci. U.S.A.* **108**: 5357-5362.
584 Morgan, A. D., Quigley, B. J. Z., Brown, S. P. & Buckling, A. 2012. Selection on non-social
585 traits limits the invasion of social cheats. *Ecol. Lett.* **15**: 841-846.
586 Morran, L. T., Schmidt, O. G., Gelarden, I. A., Parrsish, R. C. & Lively, C. M. 2011. Running
587 with the Red Queen: host-parasite coevolution selects for biparental sex. *Science*
588 **333**: 216-218.
589 Nadell, C. D., Xavier, J. B. & Foster, K. R. 2009. The sociobiology of biofilms. *FEMS*
590 *Microbiol. Rev.* **33**: 206-224.
591 R Development Core Team. 2015. R: A language and environment for statistical computing.
592 R Foundation for Statistical Computing, Vienna, Austria.
593 Ritchings, B. W., Almira, E. C., Lory, S. & Ramphal, R. 1995. Cloning and phenotypic
594 characterization of fleS and fleR, new response regulators of *Pseudomonas*
595 *aeruginosa* which regulate motility and adhesion to mucin. *Infect. Immun.* **63**: 4868-
596 4876.

Ross-Gillespie, A., Dumas, Z. & Kümmerli, R. 2015. Evolutionary dynamics of interlinked public goods traits: an experimental study of siderophore production in *Pseudomonas aeruginosa*. *J. Evol. Biol.* **28**: 29-39.

Ross-Gillespie, A., Gardner, A., Buckling, A., West, S. A. & Griffin, A. S. 2009. Density dependence and cooperation: theory and a test with bacteria. *Evolution* **63**: 2315-2325.

Ross-Gillespie, A., Gardner, A., West, S. A. & Griffin, A. S. 2007. Frequency dependence and cooperation: theory and a test with bacteria. *Am. Nat.* **170**: 331-342.

Rumbaugh, K. P., Trivedi, U., Watters, C., Burton-Chellew, M. N., Diggle, S. P. & West, S. A. 2012. Kin selection, quorum sensing and virulence in pathogenic bacteria. *Proc. R. Soc. B* **279**: 3584-3588.

Santorelli, L., Kümmerli, R., Toll-Riera, M., Griffin, A. S. & West, S. A. in preparation. Resistance to cheating in the bacterium *Pseudomonas aeruginosa*. *J. Evol. Biol.*

Schalk, I. J. & Guillon, L. 2013. Pyoverdine biosynthesis and secretion in P*seudomonas aeruginosa*: implications for metal homeostasis. *Environ. Microbiol.* **15**: 1661-1673.

Schulte, R. D., Makes, C., Hasert, B., Michiels, N. K. & Schulenburg, H. 2010. Multiple reciprocal adaptations and rapid genetic change upon experimental coevolution of an animal host and its microbial parasite. *Proc. Natl. Acad. Sci. U.S.A.* **107**: 7359-7364.

Smith, E. E., Sims, E. H., Spencer, D. H., Kaul, R. & Olson, M. V. 2005. Evidence for diversifying selection at the pyoverdine locus of *Pseudomonas aeruginosa*. *J. Bacteriol.* **187**: 2138-2147.

Stover, C. K., Pham, X. Q., Erwin, A. L., Mizoguchi, S. D., Warrener, P., Hickey, M. J., Brinkman, F. S. L., Hufnagle, W. O., Kowalik, D. J., Lagrou, M., Garber, R. L., Goltry, L., Tolentino, E., Westbrock-Wadman, S., uan, ., Brody, L. L., Coulter, S. N., Folger, K. R., Kas, A., Larbig, K., Lim, R., Smith, K., Spencer, D., Wong, G. K. S., Wu, Z., Paulsen, I. T., Reizer, J., Saier, M. H., Hancock, R. E. W., Lory, S. & Olson, M. V. 2000. Complete genome sequence of *Pseudomonas aeruginosa* PAO1, an opportunistic pathogen. *Nature* **406**: 959-964.

625 Strassmann, J. E. & Queller, D. C. 2011. Evolution of cooperation and control of cheating in
626 a social microbe. *Proc. Natl. Acad. Sci. U.S.A.* **108**: 10855-10862.
627 Thrall, P. H., Laine, A.-L., Ravensdale, M., Nemri, A., Dodds, P. N., Barrett, L. & Burdon, J. J.
628 2012. Rapid genetic change underpins antagonistic coevolution in a natural host-
629 pathogen metapopulation. *Ecol. Lett.* **15**: 425-435.
630 Tiburzi, F., Imperi, F. & Visca, P. 2008. Intracellular levels and activity of PvdS, the major iron
631 starvation sigma factor of *Pseudomonas aeruginosa*. *Mol. Microbiol.* **67**: 213-227.
632 Velicer, G. J., Kroos, L. & Lenski, R. E. 1998. Loss of social behaviors by *Mysococcus*
633 *xanthus* during evolution in an unstructured habitat. *Proc. Natl. Acad. Sci. U.S.A.* **95**:
634 12376-12380.
635 Velicer, G. J. & Vos, M. 2009. Sociobiology of the *Myxobacteria*. *Annu. Rev. Microbiol.* **63**:
636 599-623.
637 Waite, A. J. & Shou, W. 2012. Adaptation to a new environment allows cooperators to purge
638 cheaters stochastically. *Proc. Natl. Acad. Sci. U.S.A.* **109**: 19079-19086.
639 West, S. A., Diggle, S. P., Buckling, A., Gardner, A. & Griffin, A. S. 2007. The social lives of
640 microbes. *Annu. Rev. Ecol. Evol. Syst.* **38**: 53-77.
641 West, S. A., Griffin, A. S., Gardner, A. & Diggle, S. P. 2006. Social evolution theory for
642 microorganisms. *Nat. Rev. Microbiol.* **4**: 597-607.
643 Xavier, J. B., Kim, W. & Foster, K. R. 2011. A molecular mechanism that stabilizes
644 cooperative secretions in *Pseudomonas aeruginosa*. *Mol. Microbiol.* **79**: 166-179.
645 Zhang, Q.-G., Buckling, A., Ellis, R. J. & Godfray, H. C. J. 2009. Coevolution between
646 cooperators and cheats in a microbial system. *Evolution* **63**: 2248-2256.
647

Figure captions

Fig. 1 Evolutionary dynamics of cheat frequency (a), population growth (b), and pyoverdine production levels (c) in mixed populations of cooperative pyoverdine producers and non-pyoverdine-producing cheats of the bacterium *P. aeruginosa*. Experimental evolution occurred across 25 rounds of growth (approximately 150 bacterial generations). Cheat frequency first increased and then levelled off. Population growth and pyoverdine production significantly dropped over time. Grey lines depict averages across 16 replicates. Blue and orange lines show replicates in which the cooperator or cheat strain was labelled with a neutral GFP marker, respectively.

Fig. 2 Relative cheat fitness as a function of the evolutionary origin of cheats (along the x-axis) and cooperators (from a to f). Origin of both cheats and cooperators significantly affected cheat fitness, as indicated by the dashed trend lines, and the overall reduction in cheat fitness when moving from (a) to (f). These patterns suggest that cooperators from later evolutionary time points were less exploitable by cheats, and that cheats from later evolutionary time points became increasingly better at outcompeting cooperators. Blue, red and grey circles indicate combinations where cooperators competed against cheats from their past, future, and presence, respectively. Circles above or below the zero-line indicate that cheats won or lost the competition, respectively.

Fig. 3 Experiments testing for media versus social adaptations. (a) Growth of evolved clones in monocultures slightly but significantly increased over evolutionary time both for cooperators (blue lines) and cheats (green lines) indicating adaptation to the media outside the social context. (b) Analysis of the clonal pyoverdine production profiles revealed a significant drop over evolutionary time, suggesting that also the social trait of interest was under selection. (c) Evolved clones consistently outcompeted their ancestors both in iron-replete and iron-deplete environments (selection coefficient > 0). In support of the hypothesis that both social and abiotic adaptations drove the evolutionary dynamics observed in our

676 system, we found that the selection coefficient of evolved cooperators was significantly
677 higher under iron-deplete conditions, where both social and abiotic adaptations were
678 important, than under iron-replete conditions, where only abiotic adaptations matter. All
679 values in (a) and (b) are scaled relative to the ancestral wildtype, and represent means
680 across clones from the same replicate. Colour shadings depict the different replicates and
681 dashed lines represent significant trendlines.
682
683 **Fig. 4** Relationship between SNP mutations in the iron starvation sigma factor PvdS,
684 pyoverdine production and fitness of evolved cooperator clones. Evolved clones with SNPs
685 in the PvdS region (red circles) produced significantly less pyoverdine and had significantly
686 lower fitness than evolved clones without SNPs in the PvdS region (blue circles). All values
687 are scaled relative to the ancestral wildtype (dashed lines). Closed circles depict means
688 across clones from the same replicate and mutation event, while open circles represent
689 averages across replicates.
690
691 **Fig. 5** Relationship between swarming motility and fitness of evolved clones isolated at the
692 end of the evolution experiment. Swarming assays revealed that a large number of evolved
693 clones were motility impaired (red circles, $r_s < 0.75$). Evolved clones with motility impairment
694 grew marginally significantly better than the ancestral wildtype, but not different from evolved
695 strains without motility impairment (blue circles). All values are scaled relative to the
696 ancestral wildtype (dashed lines). Closed circles depict means across clones from the same
697 replicate and mutation event, while open circles represent averages across replicates.
698

Supporting Information

Additional Supporting Information may be found in the online version of this article:

Figure S1 Continuous linear growth of ancestral cooperator (blue line) and cheat (red line) monocultures in iron-depleted CAA medium. Solid and dotted lines depict mean and 95% confidence intervals across 24 replicates, respectively.

Figure S2 At the end of the evolution experiment, the evolved community level pyoverdine production (a) and population growth (b) were significantly negatively correlated with the proportion of cheats, showing that cheat accumulation first drives cooperation and then the entire population to extinction. Dashed lines indicate trend lines. Filled and open circles represent replicates in which the cooperator or cheat strain was labelled with a neutral GFP marker, respectively.

Table S1 Non-synonymous and intergenic SNPs in evolved cooperator and cheat clones

Table S2 SNPs of the PAO1 wildtype strain used in this study compared to the reference PAO1-UW (http://pseudomonas.com)

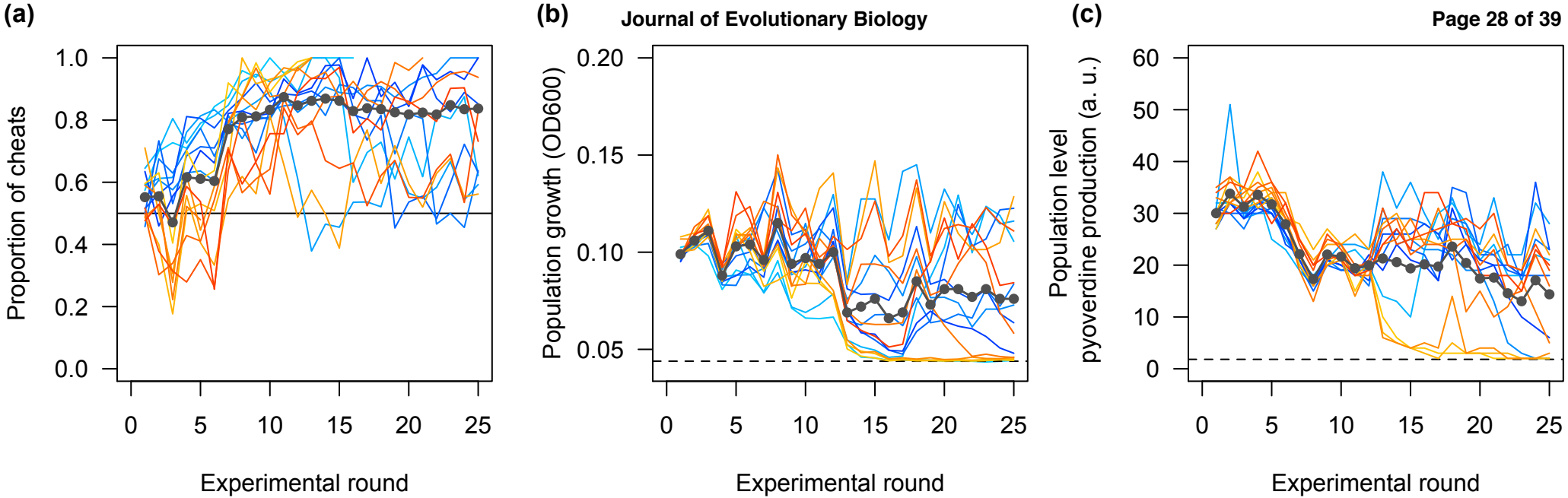
(a)
Proportion of cheats
1.0
0.8
0.6
0.4
0.2
0.0
0
5
10
15
20
25
Experimental round
(b)
Population growth (OD600)
0.20
0.15
0.10
0.05
0
5
10
15
20
25
Experimental round
(c)
Population level pyoverdine production (a. u.)
60
50
40
30
20
10
0
0
5
10
15
20
25
Experimental round

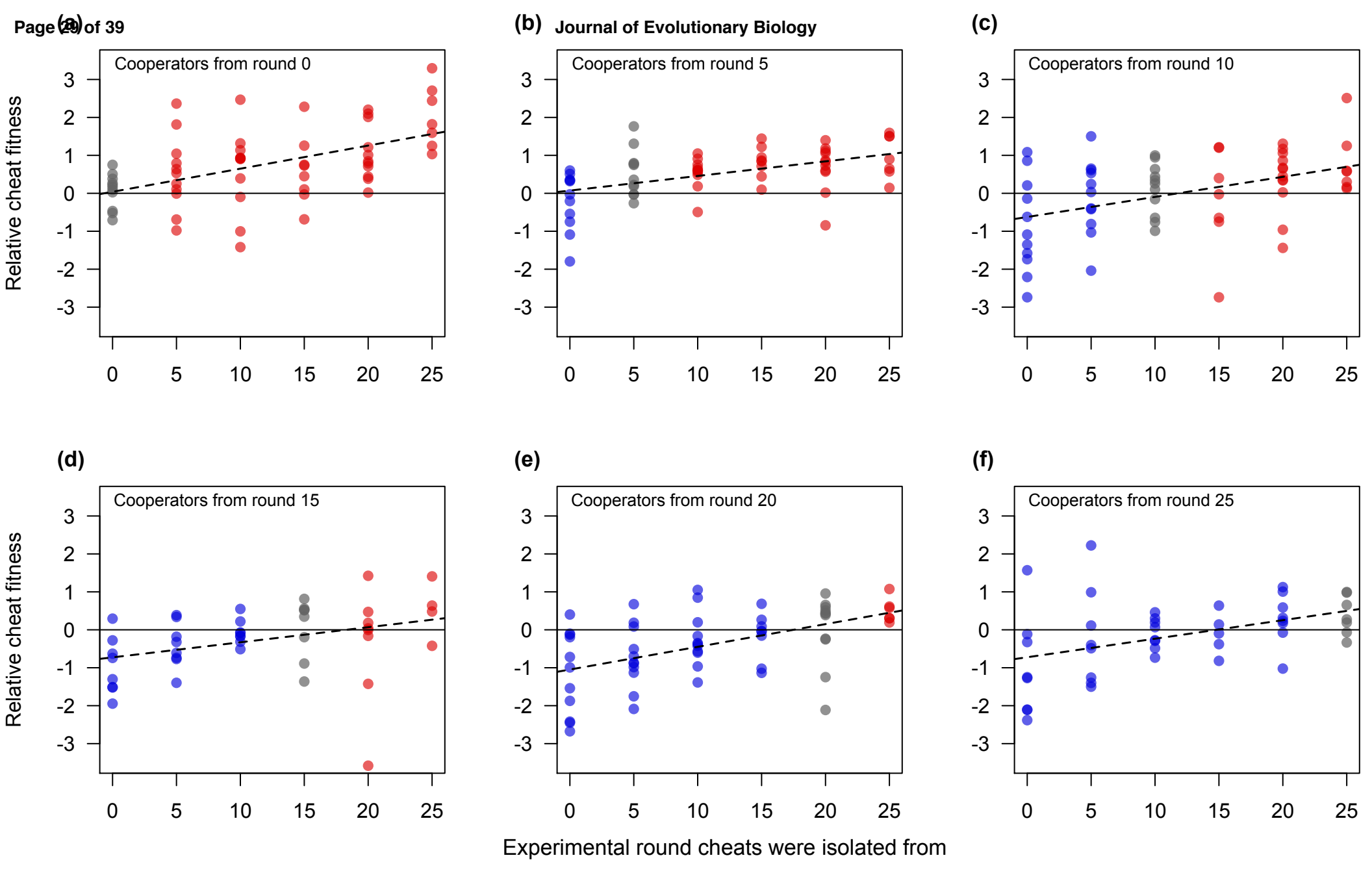
(a)
Cooperators from round 0
(b)
Cooperators from round 5
(c)
Cooperators from round 10
(d)
Cooperators from round 15
(e)
Cooperators from round 20
(f)
Cooperators from round 25
Relative cheat fitness
Relative cheat fitness
Experimental round cheats were isolated from

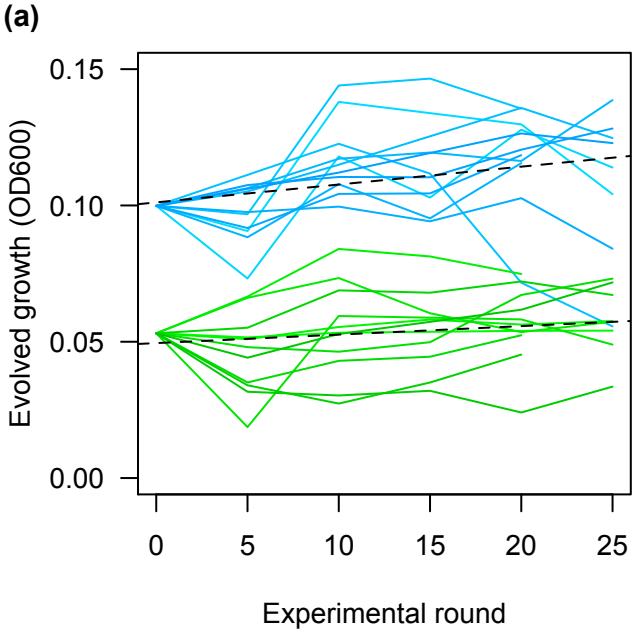
(a)
Evolved growth (OD600)
0.15
0.10
0.05
0.00
0
5
10
15
20
25
Experimental round

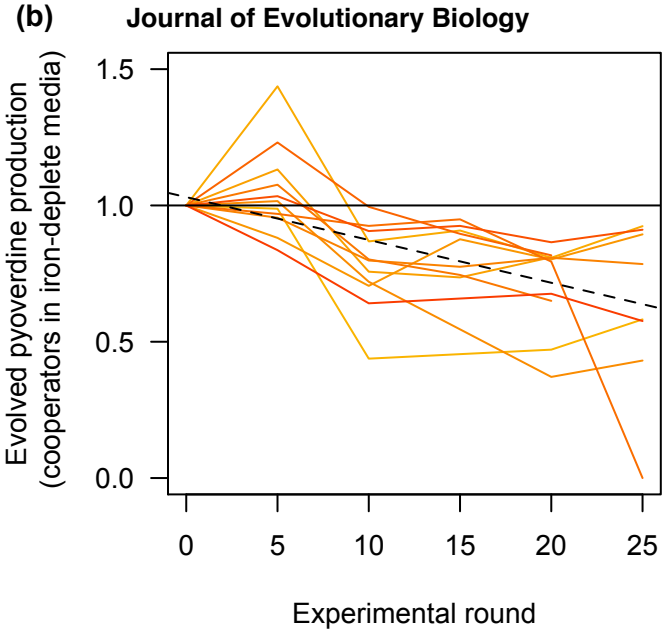
(b)
Evolved pyoverdine production
(cooperators in iron-deplete media)
1.5
1.0
0.5
0.0
0
5
10
15
20
25
Experimental round

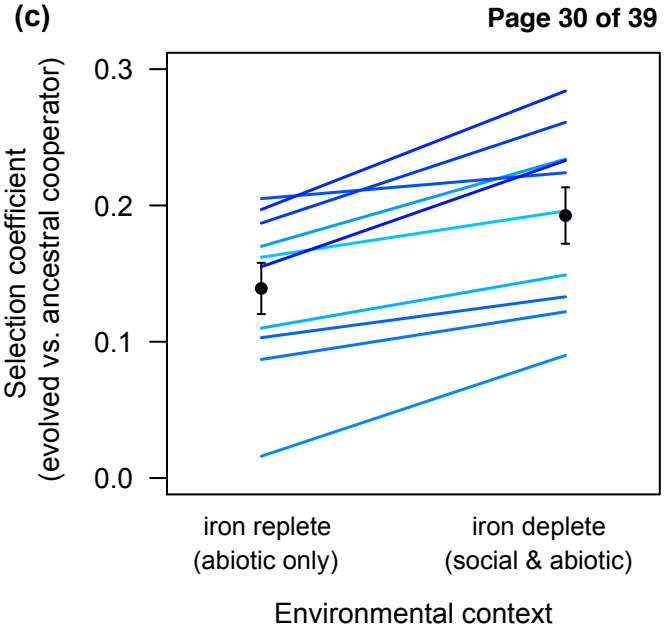
(c)
Selection coefficient
(evolved vs. ancestral cooperator)
0.3
0.2
0.1
0.0
iron replete
(abiotic only)
iron deplete
(social & abiotic)
Environmental context

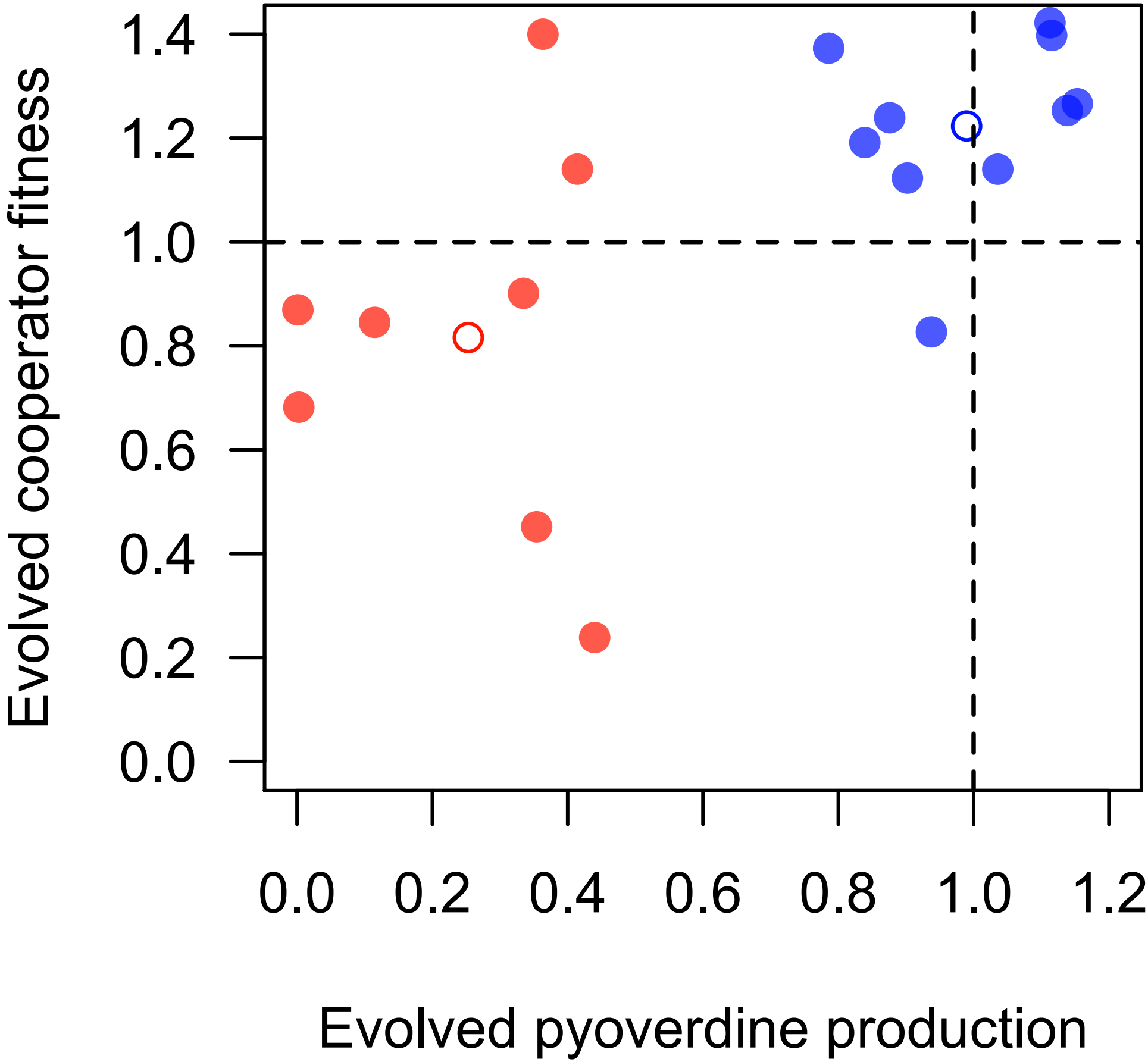
Evolved cooperator fitness
1.4
1.2
1.0
0.8
0.6
0.4
0.2
0.0
0.0
0.2
0.4
0.6
0.8
1.0
1.2
Evolved pyoverdine production

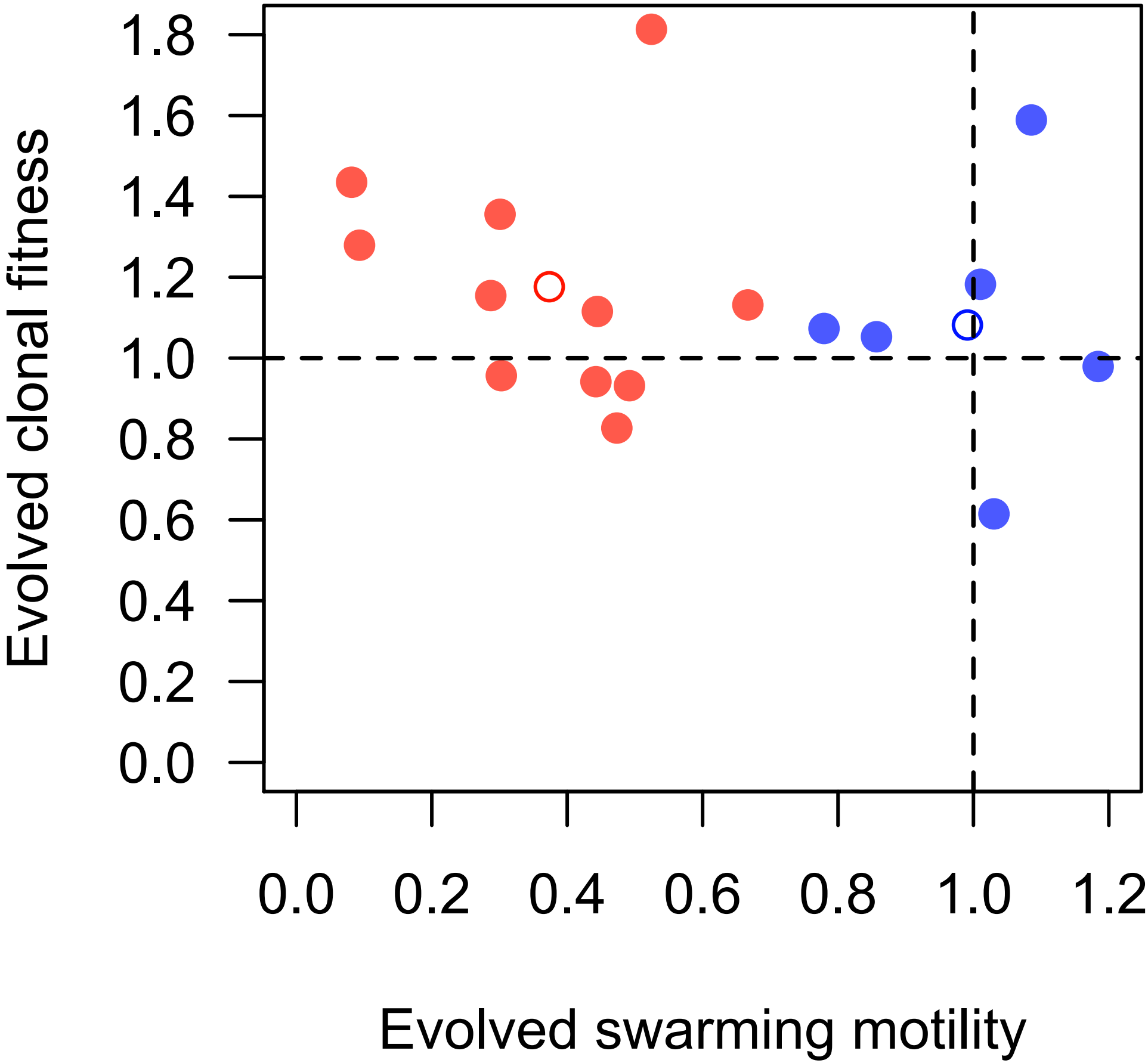
Evolved clonal fitness
1.8
1.6
1.4
1.2
1.0
0.8
0.6
0.4
0.2
0.0
0.0
0.2
0.4
0.6
0.8
1.0
1.2
Evolved swarming motility

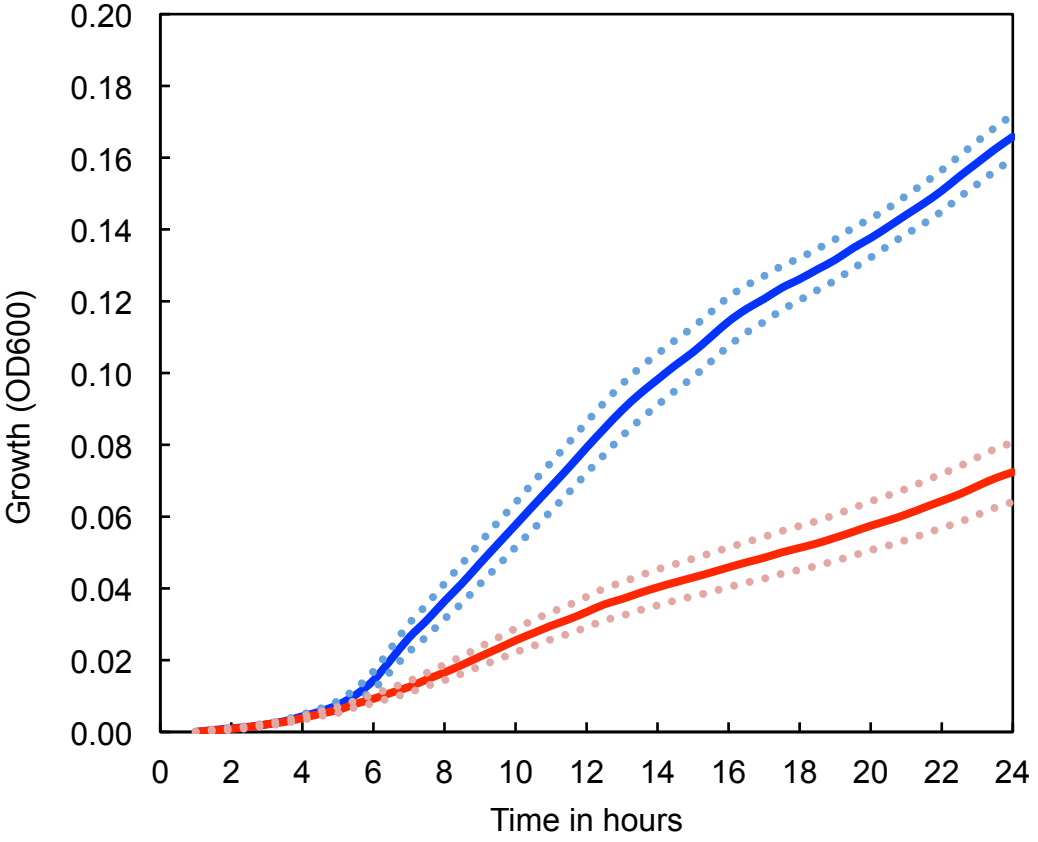
0.20
0.18
0.16
0.14
0.12
0.10
0.08
0.06
0.04
0.02
0.00
Growth (OD600)
0
2
4
6
8
10
12
14
16
18
20
22
24
Time in hours

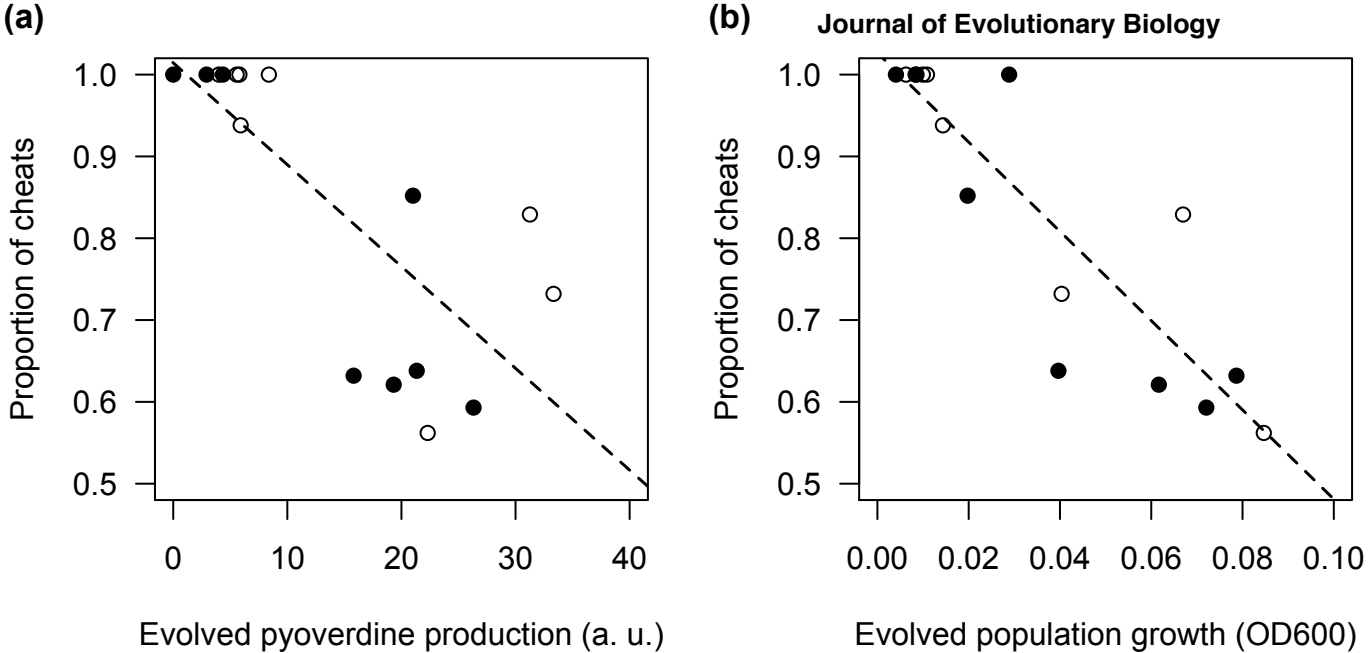
(a)
(b)
Proportion of cheats
1.0
0.9
0.8
0.7
0.6
0.5
0
10
20
30
40
Evolved pyoverdine production (a. u.)
0.00
0.02
0.04
0.06
0.08
0.10
Evolved population growth (OD600)

Table S1 Non-synonymous and intergenic SNPs in evolved cooperator and cheat clones (see below for color code)

replicate ID	strain	sequence pool	clones pooled	position	locus tag	gene	function	reference nucleotide	mutation nucleotide	amino acid change	frequency mutation	coverage
2	cooperator	seq02	2	2722485	PA2426	pvdS	iron starvation sigma factor	C	T	Ser104Leu	1.000	167
		seq01	5	1581399	PA1452	flhA	flagellar biosynthesis protein	T	A	Leu360Gln	0.468	188
		seq01	5	6258906	PA5565	gidA	glucose-inhibited division protein A	G	T	Gln98Lys	0.102	157
	cheat	seq03	10	1168303	PA1082	flgG	flagellar basal-body rod protein	T	G	Val7Gly	0.596	225
		seq03	10	1590403	PA1459	hypothetical	probable chemotaxis signal transduction methyltransferase	C	T	Leu356Phe	0.300	217
		seq03	10	5051522	PA4513	hypothetical	probable oxidoreductase	G	C	Arg627Gly	0.104	164
3	cooperator	seq04	7	1590022	PA1459	hypothetical	probable chemotaxis signal transduction methyltransferase	G	A	Ala229Thr	0.215	158
		seq04	7	1590025	PA1459	hypothetical	probable chemotaxis signal transduction methyltransferase	G	A	Glu230Lys	0.191	162
		seq04	7	1586410	PA1457	cheZ	chemotaxis protein	A	C	His126Pro	0.158	202
		seq04	7	1192834	PA1101	fliF	flagella M-ring outer membrane protein precursor	T	C	Phe144Leu	0.134	186
	cheat	seq05	5	1192834	PA1101	fliF	flagella M-ring outer membrane protein precursor	T	T	Phe144Leu	0.395	205
		seq05	5	1580235	NA	intergenic	upstream of flagellar biosynthesis protein FlhA	A	G	NA	0.220	209
		seq05	5	118825	PA0097	hypothetical	unknown	G	A	Gly299Ser	0.205	303
		seq05	5	4776647	PA4270	rpoB	DNA-directed RNA polymerase beta chain	A	T	Val1324Glu	0.156	333
		seq05	5	3650180	PA3262	hypothetical	probable peptidyl-prolyl cis-trans isomerase, FkbP-type	G	C	Ala96Gly	0.117	128
4	cooperator	seq06	4	1570790	PA1441	fliK	putative flagellar hook-length control protein	C	T	Gln99*	0.515	204
		seq06	4	3762307	PA3350	hypothetical	flagellar basal body P-ring biosynthesis protein	T	C	Leu116Pro	0.243	226
	cheat	seq07	10	1030269	PA0940	hypothetical	unknown	G	C	Ala48Gly	0.238	244
		seq07	10	3888238	PA3475	pheC	cyclohexadienyl dehydratase precursor	C	A	Leu249Phe	0.133	128
		seq07	10	1433126	NA	intergenic	upstream of probable TonB dependent receptor	C	A	NA	0.131	236
		seq07	10	4246263	PA3789	hypothetical	uncharacterized iron-regulated membrane protein	A	C	Val459Gly	0.130	138
		seq07	10	4706190	PA2019	mexG	multidrug efflux membrane fusion protein precursor	G	C	Gly79Arg	0.114	185

replicate ID	strain	sequence pool	clones pooled	position	locus tag	gene	function	reference nucleotide	mutation nucleotide	amino acid change	frequency mutation	coverage
5	cooperator	seq08	1	1171084	PA1085	flgJ	flagellar protein	C	T	Ser48Leu	1.000	251
		seq09	6	2722637	PA2426	pvdS	iron starvation sigma factor	A	C	Thr155Pro	1.000	80
		seq09	6	4917629	NA	intergenic	upstream of GroES co-chaperonin	C	A	NA	0.178	90
	cheat	seq10	10	1191982	NA	intergenic	uptstream of flagellar hook-basal body complex protein FliE	A	G	NA	0.570	207
		seq10	10	2590446	PA2345	hypothetical	conserved hypothetical protein	G	C	Ala407Gly	0.170	94
		seq10	10	1060494	NA	intergenic	upstream of hypothetical protein	C	T	NA	0.161	279
6	cooperator	seq12	6	2722637	PA2426	pvdS	iron starvation sigma factor	A	C	Thr155Pro	1.000	83
		seq11	4	1580235	NA	intergenic	upstream of flagellar biosynthesis protein FlhA	A	G	NA	0.597	216
		seq12	6	5444367	PA4849	hypothetical	unknown	C	G	Ala39Gly	0.207	87
		seq12	6	714235	PA0660	hypothetical	dioxygenases related to 2-nitropropane dioxygenase	C	T	Ala5Thr	0.165	127
	cheat	seq13	10	1589452	PA1459	hypothetical	probable chemotaxis signal transduction methyltransferase	G	T	Glu39*	0.769	78
		seq13	10	5474135	PA4878	brlR	transcriptional regulator involved in efflux pump regulation	A	G	Ile124Val	0.185	108
		seq13	10	292176	PA0260	hypothetical	unknown	G	C	Arg377Gly	0.183	82
		seq13	10	1189979	PA1098	fleS	two-component sensor regulating motility and adhesion	C	T	Gln270*	0.181	94
		seq13	10	2722079	NA	intergenic	promoter region of iron starvation sigma factor PvdS	G	T	NA	0.158	95
7	cooperator	seq14	8	no SNPs discovered								
	cheat	seq15	10	1165379	PA1079	flgD	flagellar basal-body rod modification protein	T	G	Val80Gly	0.180	100
8	cooperator	seq17	1	2722079	NA	intergenic	promoter region of iron starvation sigma factor PvdS	G	T	NA	1.000	111
		seq16	9	4732864	PA4225	pchF	pyochelin synthetase	G	C	Ala1312Gly	0.235	68
	cheat	seq18	10	2722275	PA2426	pvdS	promoter region of iron starvation sigma factor PvdS	G	A	Gly34Asp	1.000	60

replicate ID	strain	sequence pool	clones pooled	position	locus tag	gene	function	reference nucleotide	mutation nucleotide	amino acid change	frequency mutation	coverage
11	cooperator	seq19	10	1183369	PA1092	fliC	flagellar filament protein (flagellin type B)	C	G	Asn104Lys	1.000	89
		seq19	10	2722079	NA	intergenic	promoter region of iron starvation sigma factor PvdS	G	T	NA	0.920	112
		seq19	10	25077	PA0023	qor	quinone oxidoreductase	C	G	Ala157Pro	0.213	75
		seq19	10	2722313	PA2426	pvdS	iron starvation sigma factor	T	C	Phe47Leu	0.059	85
	cheat	seq20	10	1581291	PA1452	flhA	flagellar biosynthesis protein	C	T	Ala324Val	0.491	108
		seq20	10	1589707	PA1459	hypothetical	probable chemotaxis signal transduction methyltransferase	G	T	Glu124*	0.237	118
		seq20	10	2722079	NA	intergenic	promoter region of iron starvation sigma factor PvdS	G	T	NA	0.202	114
14	cooperator	seq21	8	no SNPs discovered								
		seq22	2	2722079	NA	intergenic	promoter region of iron starvation sigma factor PvdS	G	T	NA	1.000	93
		seq22	2	3683814	PA3290	hypothetical	unknown	T	C	Tyr112Cys	0.532	124
	cheat	seq23	10	1590283	PA1459	hypothetical	probable chemotaxis signal transduction methyltransferase	G	A	Gly316Ser	0.909	33
15	cooperator	seq24	1	4310610	PA3849	hypothetical	unknown	C	A	Ala236Glu	1.000	74
		seq25	7	1184318	PA1092	fliC	flagellar filament protein (flagellin type B)	G	T	Ala421Ser	0.378	336
		seq25	7	1011727	PA0926	hypothetical	unknown	G	C	Ala74Gly	0.156	128
		seq25	7	1022517	PA0933	ygcA	probable RNA methyltransferase	C	G	Ala301Gly	0.155	116
		seq25	7	4005940	PA3573	hypothetical	probable major facilitator superfamily (MFS) transporter	C	G	Arg69Pro	0.138	109
		seq25	7	1050271	NA	intergenic	upstream of pqsR-mediated PQS regulator	T	C	NA	0.126	135
		seq25	7	107333	PA0089	tssG1	protein secretion by the type VI secretion system	C	G	Ala51Gly	0.106	180
		seq25	7	5726985	PA5088	hypothetical	unknown	G	C	Ala85Gly	0.101	287
	cheat	seq26	10	1586742	PA1457	cheZ	chemotaxis protein	C	T	Gln237*	0.374	206
		seq26	10	2722079	NA	intergenic	promoter region of iron starvation sigma factor PvdS	G	T	NA	0.202	183
		seq26	10	3226658	PA2873	tgpA	transglutaminase protein A	C	T	Gly244Arg	0.146	199
		seq26	10	4917629	NA	intergenic	upstream of GroES co-chaperonin	C	A	NA	0.118	136
		seq26	10	5242140	NA	intergenic	unknown	T	C	NA	0.101	328

replicate ID	strain	sequence pool	clones pooled	position	locus tag	gene	function	reference nucleotide	mutation nucleotide	amino acid change	frequency mutation	coverage
16	coop	seq27	1	1193389	PA1101	fliF	Flagella M-ring outer membrane protein precursor	G	T	Gly329Trp	1.000	73
		seq28	5	1590244	PA1459	hypothetical	probable chemotaxis signal transduction methyltransferase	G	A	Ala303Thr	1.000	167
		seq29	3	2722095	NA	intergenic	promoter region of iron starvation sigma factor PvdS	C	T	NA	1.000	20
		seq28	5	3992219	PA3562	fruI	phosphotransferase system transporter enzyme I	G	T	Asp731Glu	0.293	58
		seq28	5	1050271	NA	intergenic	upstream of pqsR-mediated PQS regulator	T	C	NA	0.289	97
		seq28	5	643452	PA0585	hypothetical	hypothetical protein	G	C	Ala88Gly	0.132	152
		seq28	5	4624957	PA4135	hypothetical	probable transcriptional regulator	C	G	Arg16Pro	0.126	119
		seq28	5	5402008	NA	intergenic	upstream of fdnG -formate dehydrogenase-O, major subunit	C	G	NA	0.118	170
		seq28	5	3953659	PA3534	hypothetical	probable oxidoreductase	A	C	Val317Gly	0.113	177
		seq28	5	5950551	PA5286	hypothetical	conserved hypothetical protein	T	G	Thr102Pro	0.108	240
		seq28	5	5042244	PA4503	hypothetical	probable permease of ABC transporter	C	A	Asp59Glu	0.104	183
		seq28	5	4131732	PA3690	hypothetical	probable metal-transporting P-type ATPase	G	C	Arg66Pro	0.103	146
		seq28	5	4372668	PA3903	prfC	peptide chain release factor 3	G	C	Ala234Pro	0.101	148
	cheat	seq30	10	2722079	NA	intergenic	promoter region of iron starvation sigma factor PvdS	G	T	NA	0.647	153
		seq30	10	1590253	PA1459	hypothetical	probable chemotaxis signal transduction methyltransferase	C	T	Leu306Phe	0.173	133
		seq30	10	1590218	PA1459	hypothetical	probable chemotaxis signal transduction methyltransferase	C	A	Ala294Asp	0.130	131

Color code

SNPs in pvdS region

SNPs in flagella genes or putative regulatory sequences

SNPs in chemotaxis genes

other SNPs

Table S2 SNPs of the PAO1 wildtype strain used in this study compared to the reference PAO1-UW

position	locus tag	gene	function	reference nucleotide	mutation nucleotide	amino acid change	frequency mutation	coverage
non-synonymous SNPs								
183697	PA0159	hypo-thetical	probable transcriptional regulator	T	G	Cys310Trp	1.000	372
1589438	PA1459	hypo-thetical	probable chemotaxis signal transduction methyltransferase	G	C	Gly34Ala	1.000	285
2669175	PA2400	pvdJ	non-ribosomal peptide synthetase involved in pyoverdine synthesis	G	C	Pro819Ala	1.000	249
2807982	PA2492	mexT	transcriptional regulator	T	A	Phe172Ile	1.000	149
2808180	PA2492	mexT	transcriptional regulator	C	A	Pro238Thr	1.000	153
4212201	PA3760	NA	N-Acetyl-D-Glucosamine phosphotransferase system transporter	A	G	His636Arg	1.000	207
4869855	PA4341	hypo-thetical	probable transcriptional regulator	T	G	Glu158Asp	1.000	249
4924552	PA4394	hypo-thetical	unknown	C	G	Val178Leu	0.939	230
5743462	PA5100	hutU	urocanase	G	C	Thr431Arg	0.930	185
6115455	PA5434	mtr	tryptophan permease	T	G	Lys286Asn	1.000	340
synonymous SNPs								
4344266	PA3877	narK1	nitrite extrusion protein 1	A	G		1.000	185
4924553	PA4394	hypo-thetical	unknown	G	C		0.964	225
5743461	PA5100	hutU	urocanase	C	G		0.956	180
6079222	PA5399	dgcB	oxidoreductase involved in dimethylglycine catabolism	A	G		1.000	242
6098781	PA5418	soxA	sarcosine oxidase alpha subunit	G	C		1.000	283
intergenic SNPs								
413850	NA	NA	NA	T	C		1.000	119
721611	NA	NA	NA	C	T		1.000	127
721622	NA	NA	NA	C	T		1.000	136
721718	NA	NA	NA	A	G		0.992	129
721725	NA	NA	NA	C	T		0.990	105
721740	NA	NA	NA	C	T		1.000	98
2239547	NA	NA	NA	T	G		1.000	177
4448855	NA	NA	NA	C	G		1.000	58
4448856	NA	NA	NA	G	C		1.000	59
5036891	NA	NA	NA	A	C		1.000	312